

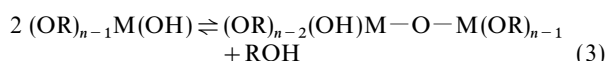
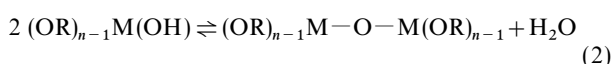
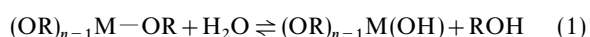
Poly(tetraethylene glycol malonate)–titanium oxide hybrid materials by sol–gel methods

Changsheng Deng, Peter F. James and Peter V. Wright*

Department of Engineering Materials, University of Sheffield, Mappin Street, Sheffield, UK S1 3JD

Hybrid materials have been prepared through the sol–gel route from poly(tetraethylene glycol malonate) (PTEGM) and titanium isopropoxide (TIP) in acidic media. The bulk gels were characterised by thermal analysis (TG, DSC and TMA), wide-angle X-ray scattering (WAXS), transmission electron microscopy (TEM) and FTIR. The results indicate that the gel incorporates –Ti–O–Ti– crosslinks appended to the dicarbonyl functions of the malonate units. The deformation temperature increases from *ca.* –50 °C to *ca.* 200 °C for $1 \geq [\text{TIP}]/[\text{TEGM}] \geq 0$. The gels are optically clear for $[\text{TIP}]/[\text{TEGM}] < 1$. For $0.5 \leq [\text{TIP}]/[\text{TEGM}] \leq 1$ TEM shows that particles ≤ 5 nm are present. At higher TIP concentration ($> ca.$ 18 mass%) the gels become slightly opaque. WAXS showed that in all the gels (< 200 °C) the titania incorporated in crosslinks or in particles was present as non-crystalline material.

Preparations of metal oxides by low temperature procedures ('sol–gel' route) have commonly involved the hydrolysis of metal alkoxides and subsequent condensation to the covalent network.

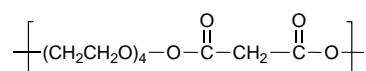


where M = Si, Ti, Zr, Al, *etc.*; R = alkyl; and *n* is the valency of the metal M. The so-called 'olation' reactions involving exchanges of coordination bonds with water or alcohol are also described in the literature.¹ Propagation of such low temperature reactions may result in fully inorganic metal–oxo networks with a high degree of homogeneity.¹ Such procedures are particularly appropriate to thin coatings. Sol–gel coatings of titania, for example, have been applied to sunlight-reflecting windows² and are proposed for bio-compatible coatings on artificial bone implants³ or as electroactive layers in electrochromic devices.⁴ However, whilst thin layers ($< ca.$ 0.5 μm in thickness) and particulate materials are readily prepared the fabrication of bulk glass or ceramic samples by these procedures is more problematic owing to the problems of shrinkage and cracking associated with the elimination of volatiles.⁵

In recent years there has been considerable interest in the preparation of organic–inorganic hybrid materials using 'sol–gel' methods.^{6–10} The incorporation of flexible organic polymer segments can greatly alleviate problems of shrinkage and cracking, so creating large-volume nano- or micro-composites of inorganic particles anchored to or dispersed within the organic matrix. Two broad classes of hybrid materials have been described.^{8,10} In 'Class I' materials the organic and inorganic phases are combined by simple mixing or permeation processes which may be followed by polymerisation of either the organic or inorganic phases, or of both, to give interpenetrating networks. An example of the latter kind of material would arise from the hydrolysis of a metal alkoxide bearing a polymerisable unsaturated function R [see eqn. (1) and (2)] such as ethylenemethacrylate.¹¹ The bonding between organic and inorganic phases is secondary in nature (*e.g.* van der Waals or hydrogen bonds). The preparation of so-called 'Class II' hybrid materials involves the use of organic polymers or polymerisable monomeric material bearing strong chelating

ligands. Examples of such ligands which form hydrolytically stable covalent bonds with transition metals following reaction with their alkoxides include salicylates and β -diketone acetylacetones or the related ethylacetoacetates which undergo keto–enol tautomerism. These ligands have been attached to polymerisable unsaturated groups such as methacrylates in the preparation of Class II materials.¹²

Here, we have explored the possibility of employing the malonic ester group as a coordinating chelate. Although it is well known that the enol form occurs in much lower quantities in malonic ester than in the β -diketones or β -keto esters, in the presence of bases the enolates are readily formed.¹³ We have not traced any reports of the use of malonic ester systems in the context of sol–gel chemistry although for hybrid materials they should have the advantage of ready incorporation into linear polyesters. In this work, a linear polyester incorporating tetraoxyethylene structural units has been prepared in order to investigate the malonate unit as a reactive chelate in hybrid materials with a metal alkoxide, titanium isopropoxide.



Such a unit is highly flexible yielding polymers of low glass transition and melting temperatures and so giving a sensitive indication of the influence of the metal chelating structure on the deformation properties of the hybrid. Furthermore, the oxyethylene segments may be doped with a lithium salt, the extent of network formation being reflected in the level of ionic conductivity of the gel. Such materials point to applications as mixed conductors in electroactive devices.

Experimental

Preparation of poly(tetraethylene glycol malonate)

Tetraethylene glycol (Aldrich) was dried over MgSO_4 and decanted before use, diethyl malonate (Aldrich) and titanium isopropoxide (Aldrich) were used as supplied.

The synthesis of poly(tetraethylene glycol malonate) (PTEGM) was adapted from ref. 14 in a two-step reaction. Tetraethylene glycol (1.2 mol) and diethyl malonate (1.0 mol) were heated in a flask under a N_2 atmosphere at 150 °C, with the titanium isopropoxide (TIP) (0.5 mass%) as the catalyst, until the evolution of ethanol had ceased. The temperature

was then increased to 220 °C and vacuum was applied and the mixture heated for a further 5 h. The poly(tetraethylene glycol malonate) was then extracted with isopropyl alcohol to remove the residual tetraethylene glycol and diethyl malonate. Finally, the polymer was dried under vacuum by repeated freeze-drying. The molar mass of the polymer was investigated by gel permeation chromatography using a calibration curve prepared from polystyrene standards. The peak molecular mass was found to be 5000 but with a polydispersity of 4.319.

Preparation of gels with titanium isopropoxide

Sols having a range of composition $0.67 \leq [\text{TEGM}]/[\text{TIP}] \leq 4$, where $[\text{TEGM}]$ is the overall concentration of polyester repeating units and $[\text{TIP}]$ is the overall concentration of titanium isopropoxide, were prepared in a solvent mixture of chloroform–isopropyl alcohol (1:1). However, two series of sols were prepared as shown in Table 1. The series A1–4 had a constant concentration of malonate units and the series B1–4 had a constant concentration of titanium isopropoxide.

As an example of such a preparation (A3) 3.5 g of polymer was dissolved in 12.7 g of cosolvent of chloroform–isopropyl alcohol (1:1, m/m). To the polymer solution, 3.8 g of $\text{Ti}(\text{OPr}^i)_4$ was added. The four-component solution was then agitated and heated on a hot plate at 50 °C for 24 h in a sealed bottle.

In order to prepare the gel a 10% solution of aqueous 0.25 M HCl in isopropyl alcohol was added dropwise to the sol to give a molar ratio $[\text{H}_2\text{O}]/[\text{TIP}] = 4$ throughout all samples. After stirring for several min the solutions were then allowed to stand at room temperature in a sealed bottle until gelation was observed when a magnetic stirrer-follower ceased to rotate. This process took between several min for the highest TIP concentration, A4, and several h for sample A1. The bottles were then opened to allow solvent to evaporate from the gels. The gels were then subdivided and a sample of each gel was heat-treated in air for 1 h at 40, 120, 150 and 200 °C. Samples A2, A3 and A4 were also heat treated at 335, 400 and 600 °C prior to analysis by wide-angle X-ray diffraction.

Characterisation

All gels prepared from the sols of Table 1 were analysed using FTIR spectroscopy using a Perkin Elmer Spectrum 2000 spectrometer. Thermogravimetry (TG) was performed using a Stanton-Redcroft TG 770 instrument and differential scanning calorimetry (DSC) and thermomechanical analysis (TMA) were carried out using a Du Pont 910 DSC and 943 TMA. Samples of hybrid materials for TMA were approximately cubic in shape of dimension *ca.* 0.5 cm; polymer-free samples were *ca.* 0.3 cm. The crystallisation behaviour of samples A2, A3 and A4 after the various heat treatments at high temperatures was monitored using wide angle X-ray diffraction (WAXS). A Philips PW 1710 diffractometer using Cu-K α radiation was employed for this purpose. ^{13}C NMR spectroscopy was performed on a Bruker AMX2-400 instrument. Samples for NMR analysis were prepared from 0.1 g of a mixture of TIP and PTEGM in the composition ratio of sample A2 dissolved in 0.7 ml of CDCl_3 . A Philips 400EM transmission electron microscope was employed for the observation of the microstructure of the gels. Samples were prepared by dropping several microlitres of hydrolysed sol onto carbon-

coated copper grids which were allowed to dry at room temperature.

Preparation of complexed gels with LiClO_4 and conductivity measurements

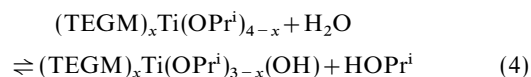
LiClO_4 was incorporated into gels composition A1 and A3 by adding the salt to the PTEGM–TIP solution in isopropyl alcohol–chloroform. The LiClO_4 was added with stoichiometry $[\text{ether oxygen}]/[\text{LiClO}_4] = 20$. A coating of gel (60 μm) was deposited onto an ITO electrode with a cellulose acetate spacer and allowed to cure in the atmosphere at room temperature for 24 h. It was dried by storage in a dessicator under vacuum.

Conductivity measurements were performed between ITO electrodes over a temperature range from 20 to 120 °C by complex impedance analysis using a Solartron 1286 Electrochemical Interface coupled to a 1250 Frequency Response Analyser.

Results and Discussion

Gelation

The polyester PTEGM is not soluble in isopropyl alcohol, which is, however, a good solvent for titanium isopropoxide. A mixed solvent of chloroform and isopropyl alcohol was therefore used. The ratio of the two solvents influences the hydrolysis and gelation kinetics. With increase in the proportion of isopropyl alcohol, the gel time increases since the 'back reaction' in the following equilibrium is promoted.



where $x = 1$ or 2 and TEGM denotes the polyester repeating unit.

In view of the constraints of solubility of both reagents and the gelation reaction rate it was found that a mixed solvent consisting of equal masses of chloroform and isopropyl alcohol was satisfactory for all compositions.

With the increase of the concentration of TIP (Table 1, samples A1–4), the gelation time decreases from 5 h to (A1) to 3 min (A4) [$\log(\text{gel time})$ vs. TIP concentration is approximately linear]. However, at constant TIP concentration (B1–4), there is much less dependence on polymer concentration in the gelation times which, like sample A2, are approximately 1 h.

The gels are all transparent except for sample A4 which has a cloudy appearance. Presumably the chelation of titanium by the polymer and the hydrolysis of TIP to form TiO_2 particles are competing reactions. With increase in concentration of TIP the reaction sites on the polymer appear to become saturated (in sample A3 there is a 1:1 equivalence of TIP and the repeating unit of the polyester). In sample A4 the direct hydrolysis of TIP to TiO_2 particles, either associated with polymer-coordinated titanium or as independent particles, presumably becomes the most dominant reaction. Although there is likely to be some uncertainty in the measurement of the faster gel times the similarity in the gel times for samples A3 and A4 is consistent with this supposition.

Table 1 Compositions and gel times of sols

	A1	A2	A3	A4	B1	B2	B3	B4
P(TEGM) (%)	18.87	17.48	17.48	17.31	6.7	9.3	19	37
TIP (%)	5.39	9.62	18.96	28.14	10	10	10	10
$[\text{TEGM}]/[\text{TIP}]^a$	3.8	2	1	0.70	0.70	1	2	4
gel time/min	310	50	3	3	80	56	50	70

^aMolar ratio.

Gel structure

Thermogravimetry (TG). Fig. 1 shows the traces of TG experiments in air for the PTEGM-TIP gel samples A1-4 which had received prior heat treatment in air at 70 °C for 24 h. Loss of mass occurs throughout heating but the most mass loss was complete at about 300 °C indicating the loss of the organic parts in the gels. After heating to 450 °C, the masses of the residues are consistent with the expected TiO₂ contents of the samples A1, A2, A3 and A4 which are 6.9, 12.3, 21.9 and 29.6%, respectively. In these calculations it has been assumed that each added mol of TIP has been converted to 1 mol TiO₂. For sample A1 the agreement is excellent but the slightly high experimental results for samples A2 and A3 and sample A4 are probably not outside the experimental error. The plots suggest that samples A3 and A4 may discharge some trapped solvents between 70 and 150 °C. (Similar solvent retention occurs in gels from pure TIP which retains *ca.* 25% of organic solvent below *ca.* 150 °C.) Greater mass retention of samples A3 and A4 above 160 °C may be attributed to the greater density of crosslinks in these samples.

Thermomechanical analysis (TMA) and differential scanning calorimetry (DSC). Thermomechanical analysis data are shown in Fig. 2 for the pure polymer PTEGM and for a series of gels prepared from [TIP]/[TEGM] molar ratios over the range 0.25 to 0.67 as well as for pure TiO₂ prepared by the sol-gel procedure. The data are presented as the percentage dimensional change, $100(L_0 - L)/L_0$ (where L_0 is the initial thickness) *versus* temperature.

The pure PTEGM shows a softening/melting process over the temperature range -50 to 0 °C. Comparison with the DSC trace [Fig. 3(a)] shows that this region corresponds to the

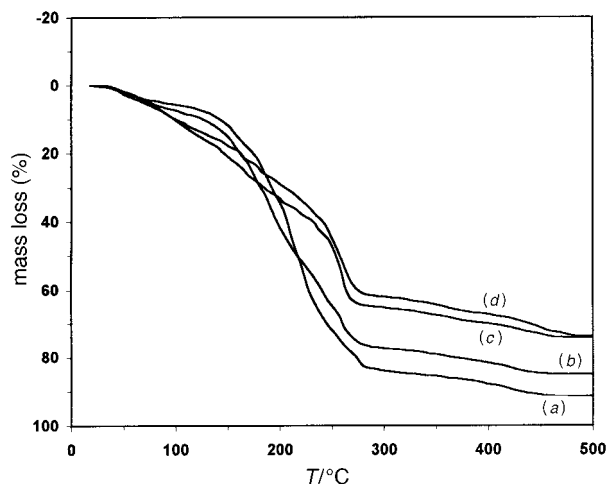


Fig. 1 Thermogravimetry (TG) traces of gels heat-treated at 70 °C for 24 h: (a) A1, (b) A2, (c) A3, and (d) A4

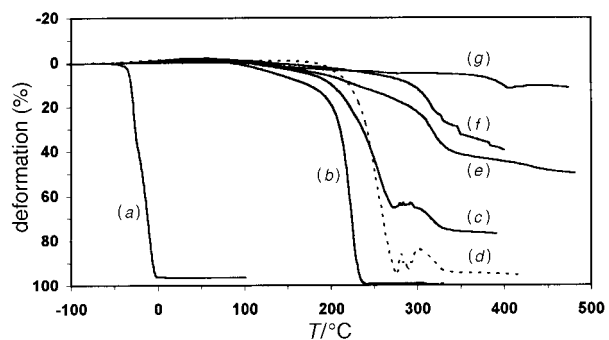


Fig. 2 Thermomechanical analysis (TMA) data of PTEGM and gels (a) PTEGM, (b) gel A1, (c) A2, (d) A2 after heat treatment at 120 °C for 24 h in air, (e) A3, (f) A4, and (g) a gel from pure TIP

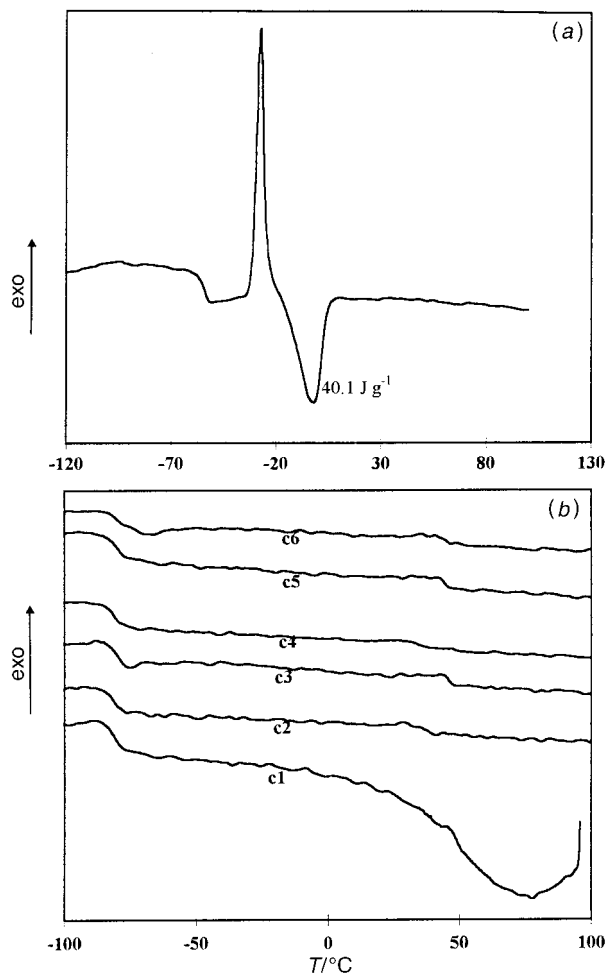


Fig. 3 Differential scanning calorimetry (DSC) traces of PTEGM and gel A2 (experiments performed in N₂): (a) PTEGM, (b) gel A2, thermal cycling (c1-c6) up to 130 °C in the DSC cell

glass transition temperature of the polymer (*ca.* -50 °C) and the melting temperature of crystalline material (T_{max} of melting endotherm is at *ca.* -1.5 °C). A small shoulder at *ca.* -25 °C may be discerned in the TMA data which presumably corresponds to the onset of melting. The heat of the endotherm (40 J g⁻¹) is low by comparison with published heats of fusion for typical aliphatic polyesters (50-90 J g⁻¹, for materials of 40-60% crystallinity) and for poly(ethylene oxide) (188.1 J g⁻¹). This is likely to be a reflection of a low degree of crystallinity as well as a low heat of fusion in the pure PTEGM.

However, Fig. 2 shows that there is a dramatic increase in the deformation temperatures of the gel with only 0.25 ([TIP]/[TEGM]). All of the gels from TIP/PTEGM show some expansion when heated above -50 °C until *ca.* 60 °C when a compressive deformation commences. The latter may indicate some solvent loss after the pretreatment at 70 °C (consistent with the TG plots of Fig. 1) and some elastic compression of the network.

The DSC tracing of a gel with TIP (sample A2), dried at room temperature and subjected to six thermal cycles in the instrument, is shown in Fig. 3(b). The T_g at -80 °C, which presumably may be attributed to the flexible polyether segments, is also apparent in the gel but there is no evidence for any crystallinity, showing that the comparatively low TIP ([TEGM]/[TIP]=2.0) is effective in disorganising the polymeric material.

However, after the first cycle to 130 °C (the endotherm at 60-70 °C presumably arises from the expulsion of chloroform) the trace becomes reproducible and shows a second, well

defined baseline shift at 50 °C. The baseline shift at 50 °C on cycles after the first coincides with the onset of significant deformation in the gels as shown in Fig. 2. It may therefore be attributed to a thermoreversible disruption of interchain interactions in the gels, presumably at the titanium coordination sites. More extended heat treatment at 120 °C overnight gives rise to a less deformable material [Fig. 2(d)]. The greater rigidity of the sample after treatment at 120 °C may presumably be attributed to more effective crosslinking by titanium interactions with the dicarbonyl functions and/or the loss of final traces of residual solvents.

Above 200 °C a more drastic breakdown of the networks is observed. Comparing the TMA and the TG data it is apparent that degradation of the organic component accounts for a high proportion of the apparent deformation above 200 °C and in sample A1 the simultaneous thermal dissociation of network crosslinks is suggested allowing the system to flow.

However, in both TMA and TG experiments there are apparent 'steps' in the deformation, and the mass loss, composition behaviour, respectively, at a composition between samples A2 ([TIP]/[TEGM]=0.5) and A3 ([TIP]/[TEGM]=1) as shown in Fig. 4. The points in Fig. 4 denote the temperatures of maximum gradients in Fig. 1 and 2. The plot suggests that at compositions between A2 and A3 a change in the nature of the organometallic crosslink may occur. This is discussed further in the next section.

¹³C NMR analysis of the polymer–titanium interaction

MAS NMR was not available to us but an investigation of a possible titanium–polymer interaction in solution in CDCl₃ (ca. 0.5 molar) having [TEGM]/[TIP]=2 has been carried out. The results for the carbonyl and central methylene carbons of the malonate residues are summarised in Table 2. The data suggest that an interaction may have occurred but the chemical shifts from pure polymer to the TIP–PTEGM mixture are

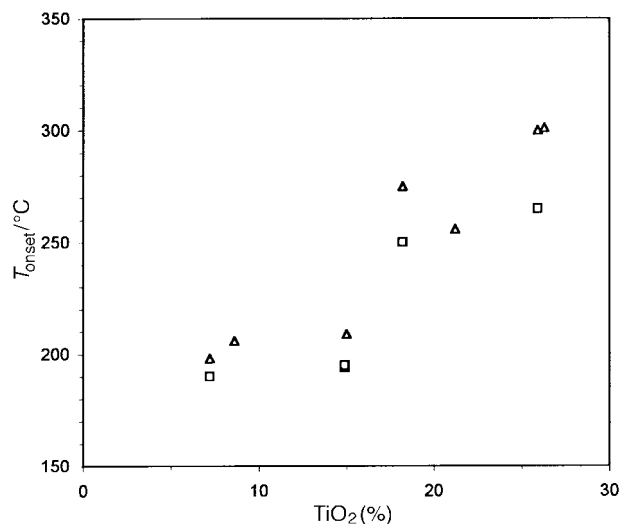


Fig. 4 Variation of temperatures of onset of deformation in TMA (□) (see Fig. 2) and of maximum gradient in TG (Δ) (data from Fig. 1 and from 'B series' gels) with TiO₂ content

much smaller than those observed for the ketonic functions of acetylacetone¹⁵ or ethylacetoacetate¹⁶ in solution. It is well known that in the absence of metal alkoxide the enol tautomer is present at much lower concentration in malonate than in the ketonic systems so that solvent stabilisation of the two components may preclude their reaction under the conditions of the NMR experiment. Meanwhile MAS NMR of the solvent-free systems are in progress. However, preliminary X-ray photoelectron spectroscopy investigations of solvent-free gels, to be reported elsewhere,¹⁷ have indicated that Ti–O bonds are formed from enolisation of the carbonyl functions.

FTIR analysis of gel structure

Fig. 5(a) shows an FTIR spectrum for pure PTEGM at room temperature. There is a strong band at 1734 cm⁻¹ which is assigned to the stretching mode of the carbonyl double bond. There are also prominent peaks at 2871 and 1137 cm⁻¹ which may be assigned to C–H stretch and C–O (ether) stretching modes, respectively.

Fig. 5(b)–(d) shows FTIR spectra for gel A3 (prepared from equimolar proportions of TIP and repeating units of the PTEGM) after heat treatments, each for 1 h, at 20, 120 and 150 °C. The most noticeable feature is the decrease in intensity of the carbonyl stretch absorption (ca. 1729 cm⁻¹) in relation to the other strong bands at ca. 1100 cm⁻¹ (C–O stretch) and 2871 cm⁻¹ (C–H stretch) if the pure polymer [Fig. 5(a)] and metal-containing systems [Fig. 5(b)–(d)] are compared. These two 'reference' bands appear to have approximately the same relative intensities as in the pure polymer. Comparing with Fig. 5(a) the O–H stretch band in the region 3320 cm⁻¹ becomes less intense with heat treatment. This trend may presumably be explained by the presence of free isopropyl alcohol and water in the gels at lower temperatures which are expelled with heating.

The peak at ca. 1630 cm⁻¹ (decreasing with heat treatment of the hybrid material) may possibly be assigned to angular bending of water; the band at 1567 cm⁻¹ (increasing with heat treatment of the hybrid) perhaps indicates the unsaturation within the malonate group arising from enolisation as the C–O–Ti bonds are formed (see structures I and II). It is noted that medium-to-strong bands in this region have been assigned to metal chelates of the 1,3-diketones¹⁸ and

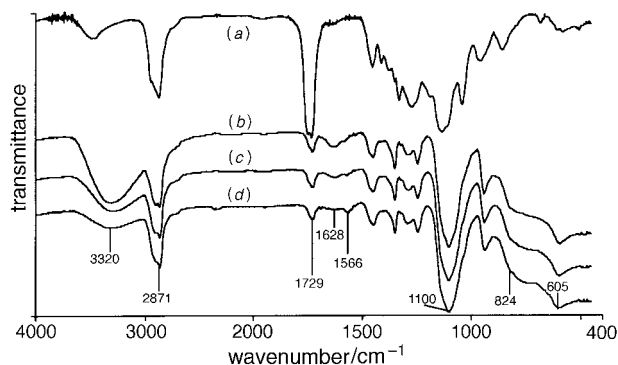
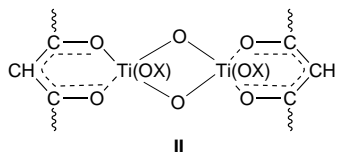
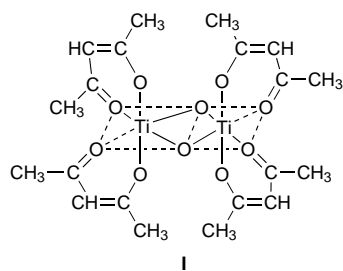


Fig. 5 FTIR spectra of (a) PTEGM, (b) gel A3 at 20 °C, and after heating for 1 h in air at (c) 120 °C and (d) 150 °C

Table 2 ¹³C NMR chemical shifts (δ) of carbons in malonate group

carbon	diethyl malonate	PTEGM	PTEGM–TIP
–O–(C=O)–CH ₂ –(C=O)–O–	41.5	41.1	41.5 42
–C=O	166.5	166.3	165.7 165.9 166.2 166.5

ketoesters.¹⁶ However, the origin of the band at 1548 cm^{-1} in the polyester-free gels [Fig. 6(b)] is unclear. It suggests that bands in this region may also be associated with unsaturated contaminants following catalysed dehydration of the secondary alcohol with heat treatment.



The IR spectrum of tributoxy titanium ethylacetoacetate has been reported by Yamamoto and Kambara.¹⁹ This spectrum does not feature a free carbonyl band in the region $1700\text{--}1750\text{ cm}^{-1}$ but there is a doublet at 1628 and *ca.* 1600 cm^{-1} assigned by Lecomte²⁰ and Bellamy and Beecher²¹ to asymmetric and symmetric vibrations of the C–O bonds which replace the carbonyls when the chelate is formed. More recently, Livage and co-workers have also observed the absence of ‘free’ carbonyl vibrations in both acetylacetonate–titanium¹⁵ and ethylacetoacetate–aluminium alkoxide¹⁶ products. Bands over the range $1530\text{--}1630\text{ cm}^{-1}$ in these materials were assigned to $\nu(\text{C}=\text{C}) + \nu(\text{C}=\text{O})$ of the enolised forms. The IR spectra of the malonate gels (Fig. 7) are thus consistent with the coordination of the titanium by the dicarbonyl functions on a diester unit (‘keto–enolisation’) The first step of this process should result in the six-membered ring involving delocalised carbonyl and alkene functions as shown in Scheme 1.

Whilst the increase in intensity of the broad band at *ca.* 1100 cm^{-1} may arise from the imposition of the O–Prⁱ vibrations onto those of the ether links within the polymer backbone, the band at 605 cm^{-1} has been assigned¹⁵ to Ti–OPrⁱ vibrations consistent with its loss in intensity with heat treatment of the gel from pure TIP (Fig. 6). However its persistence in the hybrid environment up to 150°C (Fig. 5) would indicate that the organic substituents may be more stable in the organic medium. Furthermore, the hydrophilic polyether segments should provide not only a ‘diluent’ to further condensation of the inorganic component but also a

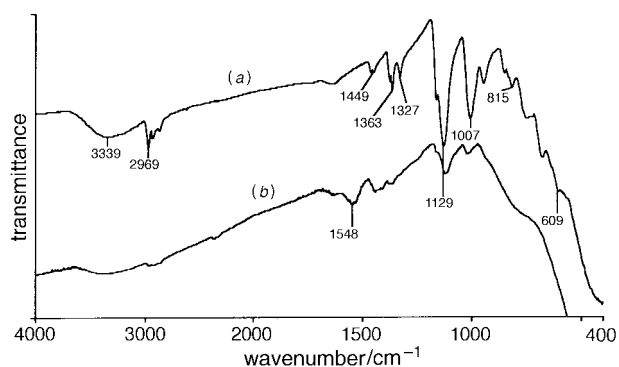


Fig. 6 FTIR spectra of a gel prepared from pure TIP: (a) room temperature dried; (b) heated at 120°C for 1 h in air

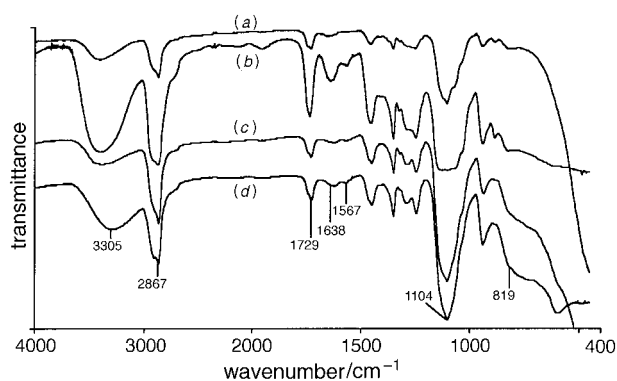
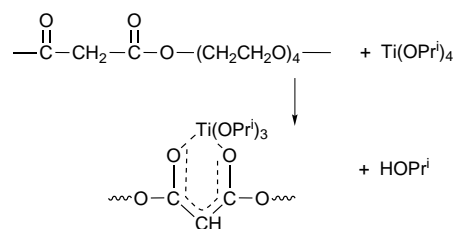


Fig. 7 FTIR spectra of gels (a) A1, (b) A2, (c) A3 and (d) A4 at room temperature



Scheme 1

stabilising environment for some unreacted water. This process would give rise to inter-malonate crosslinking and by analogy with the dimeric structure **I** for the hydrolysis product of dialkoxy–titanium bis(acetylacetonate)^{19,22} the crosslinks in the gels may be tentatively described by structure **II** where –OX may be an –OPrⁱ residue or a dicarbonyl function from a malonate residue. In the event of further development of a titania nanoparticle OX would also include Ti–OH and Ti–O–Ti.

The stoichiometry of structure **II** corresponds with that of sample A2 ($[\text{Ti}]/[\text{repeating unit}] = 0.5$) but in samples A3 and A4 the Ti is in excess. Since both A2 and A3 are apparently optically transparent any precipitation as TiO_2 must occur as submicroscopic particles in these samples. Fig. 8 shows a transmission electron micrograph of sample A2. Particles of diameter not greater than 5 nm are clearly visible in this sample. Thus formation of Ti–O–Ti links between **II** and the TiO_2 particles therefore represents another structural possibility which can account for the increased resistance to deformation of these gels. It is immediately evident that sample

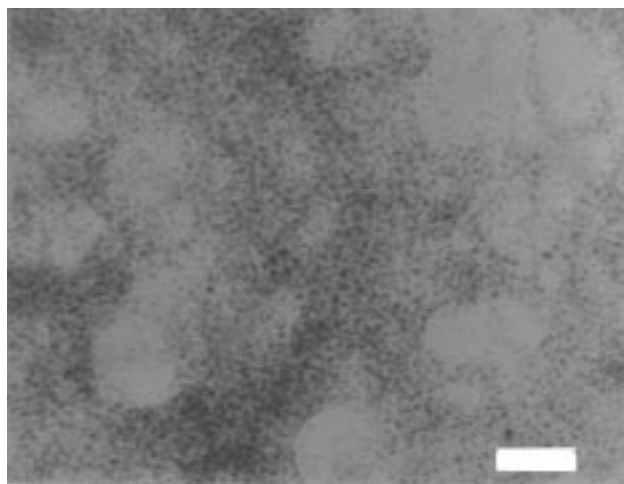


Fig. 8 Transmission electron micrograph of gel of composition A2 (scale bar is 50 nm)

A4 is slightly opaque to visible light indicating the presence of larger particles in this sample. However, in sample A1 no particles could be observed using TEM.

The broad IR bands over the range $400\text{--}700\text{cm}^{-1}$ taking in the shoulder at 824cm^{-1} are characteristic of the formation of a Ti—O—Ti network. These absorptions in the traces of Fig. 7 show a significant increase in intensity from discrete peaks in samples A1 and A2 to strong shoulders in samples A3 and A4. This observation lends some support to the TMA and TG results described above which suggested an increase in the stabilities of crosslinks on passing from sample A2 to A3.

Wide-angle X-ray diffraction

Wide-angle XRD traces of gels at room temperature and after heat treatment at various temperatures for 1 h are shown in Fig. 9. It can be seen that gels below 200°C are in the amorphous state. Samples heated at 600°C clearly show the peaks of crystalline titania. These peaks correspond to the anatase phase of titania. The samples heated at 335°C show broad peaks around the corresponding diffraction angles, the broadening of these peaks indicating the fine crystal size. These peaks seem to be well developed when temperature reaches 400°C . Therefore, the phase transition of titania commenced at *ca.* 335°C , and crystallisation was complete above 400°C . There is no apparent difference in the crystallisation behaviour between samples A2, A3, and A4 so that even in sample A4 which is slightly opaque to visible light and incorporates larger particles, the titania is deposited within the hybrid material as an amorphous phase. The absence of any discernible differences in crystallisation behaviour between titania particles within gels A2, A3 and A4 is of interest. It suggests that crystallisation is homogeneously nucleated within the particles and that the critical nucleus size for crystallisation is rather less than the size of the smallest particles (*ca.* 5 nm).

Ionic conductivity

The ionic conductivities for various PTEGM—TIP gels and for PTEGM doped with LiClO_4 are presented as $\log_{10} \sigma$ vs. $1/T$

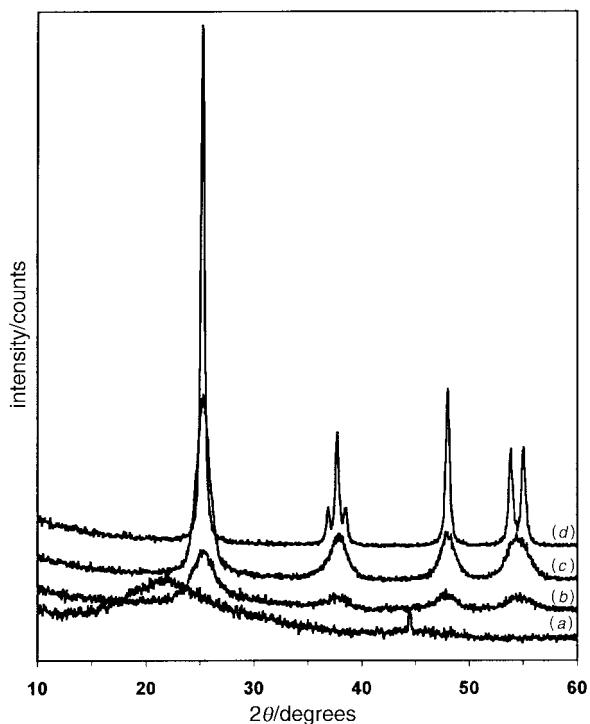


Fig. 9 Wide-angle X-ray diffraction (XRD) traces of samples from gel A2 after heat treatment in air for 1 h at (a) 200°C , (b) 335°C , (c) 400°C , and (d) 600°C

in Fig. 10. The plots are curved and typical of amorphous systems in which the charge carrier mobilities are determined by free volume mechanisms. The plot for gel A1 doped with LiClO_4 at a concentration $[\text{LiClO}_4]/[\text{TEGM}]=0.2$ is virtually indistinguishable from that for titanium-free PTEGM having the same $[\text{LiClO}_4]/[\text{TEGM}]$. Although sample A1 is a crosslinked network, the density of crosslinks is clearly insufficient to inhibit the liquid-like mobility of the polymer segments to a degree which constrains the ion mobility. The levels of conductivity of the LiClO_4 -doped A1 gel are similar to those which have been observed in other lightly crosslinked poly(ethylene oxide)-based networks.²⁴ However, the greater density of crosslinks in gel A3, doped with the same $[\text{LiClO}_4]/[\text{TEGM}]$, brings about two to three orders of magnitude reduction in conductivities. The LiClO_4 -doped A3 gel is optically transparent like its undoped counterpart. However, the conductivity data support the conclusions from the other analytical techniques that A3 is more densely crosslinked than sample A1 to a significant degree.

The gels A1 and A3, undoped with LiClO_4 , are much closer in their levels of conductivity. Their conductivities most likely arise from traces of ionic impurities. In common with doped materials the gel having the least titania content has the highest conductivity; the opposite might have been anticipated were the conductivity principally electronic. Complex impedance plots from gel A3 show well developed semicircles arising from the structural heterogeneity in the sample even though the sample is optically isotropic. The semicircle is absent in the higher conductivity LiClO_4 doped gels indicative of structural homogeneity in the conducting pathways. Work continues on other polymalonates crosslinked with inorganic particles derived from sol-gel reactions.

Conclusions

Introduction of TiO_2 into poly(tetraethylene glycol malonate) to prepare hybrid materials by the sol-gel method significantly enhances the thermomechanical properties of poly(tetraethylene glycol malonate). The materials, which are amorphous, are interconnected networks, in which poly(tetraethylene glycol malonate) chains are linked by Ti—O—Ti structures *via*

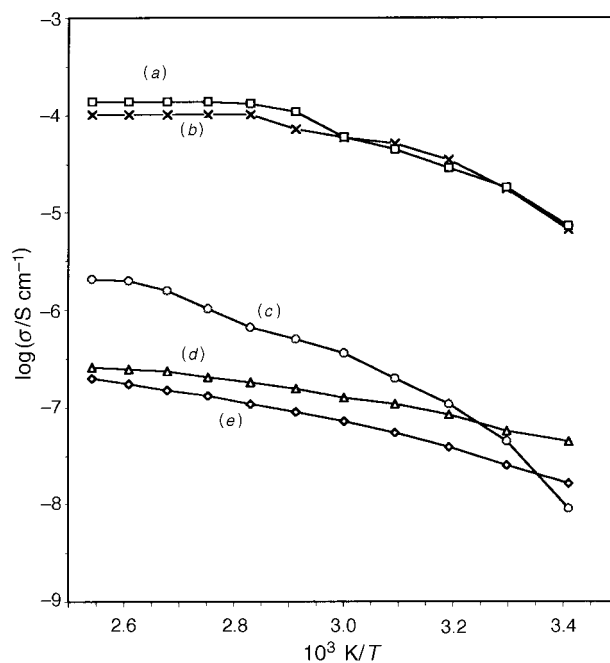


Fig. 10 Ionic conductivities of PTEGM and gels containing LiClO_4 . Molar ratios $[\text{TEGM}]:[\text{TIP}]:[\text{Li}^+]=$ (a) 20:5:4; (b) 5:0:1; (c) 5:5:1; (d) 4:1:0 and (e) 1:1:0

chelation of titanium by dicarbonyl malonate units. Gel samples prepared from reaction solutions having TIP at less than *ca.* 20 mass% were optically clear. A sample prepared from 28 mass% TIP was slightly opaque with particles estimated to be *ca.* 100 nm in size. Ionic conductivities of gels with 8.6 mass% of titania and doped with LiClO₄ were similar to that of the titania-free polymer–salt mixture. Increase in titania content brought about significant reductions in conductivities consistent with a greater densities of crosslinks.

We thank SBFSS (Sino-British Friendship Scholarship Scheme Foundation) for financial support of this project. We are also grateful to Dr B. Taylor for performing the ¹³C NMR experiments.

References

- 1 C. J. Brinker and G. W. Scherer, in *Sol–Gel Science, The Physics and Chemistry of Sol–Gel Processing*, Academic Press, San Diego, 1989.
- 2 *Prospect Calorex*[®] Das absolut farbneutrale Sonneureflexionsglas von Schott Glaswerke, Mainz, FRG, 1983.
- 3 D. B. Haddow, S. Kothari, P. F. James, R. D. Short and P. V. Hatton, *Biomaterials*, 1996, **17**, 501.
- 4 M. Nabavi, S. Doeuff, C. Sanchez and J. Livage, *Mater. Sci. Eng. B*, 1989, **3**, 203.
- 5 L. L. Hench, in *Science of Ceramic Chemical Processing*, ed. L. L. Hench and D. R. Ulrich, Wiley, New York, 1986, pp. 52–64.
- 6 B. Novak, *Adv. Mater.*, 1993, **5**, 422.
- 7 H. Schmidt, *J. Sol–Gel Sci. Technol.*, 1994, **1**, 217.
- 8 C. Sanchez and F. Ribot, *New J. Chem.*, 1994, **18**, 1007.
- 9 U. Schubert, N. Husing and A. Lorenz, *Chem. Mater.*, 1995, **7**, 2010.
- 10 P. Judeinstein and C. Sanchez, *J. Mater. Chem.*, 1996, **6**, 511.
- 11 (a) R. J. P. Corriu, D. Leclercq, A. Vioux, M. Pauthe and J. Phalippou, in *Ultrastructure Processing of Advanced Ceramics*, ed. J. D. Mackenzie and D. R. Ulrich, Wiley, New York, 1988, p. 113; (b) R. J. P. Corriu, C. Guerin and J. E. E. Moreau, *Top. Stereochem.*, 1984, 43.
- 12 C. Sanchez and M. In, *J. Non-Cryst. Solids*, 1992, **147–148**, 1.
- 13 L. Fieser and M. Fieser, in *Organic Chemistry*, Reinhold, New York, 1956, p. 221.
- 14 A. C. Tang and K. S. Yao, *J. Polym. Sci.*, 1959, **35**, 219.
- 15 A. Leautic, F. Babonneau and J. Livage, *Chem. Mater.*, 1989, **1**, 240.
- 16 L. Bonhomme-Coury, F. Babonneau and J. Livage, *J. Sol–Gel Sci. Technol.*, 1994, **3**, 157.
- 17 C. S. Deng, P. V. Wright and P. F. James, *J. Sol–Gel Sci. Technol.*, in press.
- 18 G. Socrates, in *Infrared Characteristic Group Frequencies*, John Wiley and Sons, London, 1980, p. 62.
- 19 A. Yamamoto and S. Kambara, *J. Am. Chem. Soc.*, 1957, **79**, 4344.
- 20 J. Lecomte, *Discuss. Faraday Soc.*, 1950, **9**, 125.
- 21 L. J. Bellamy and I. Beecher, *J. Chem. Soc.*, 1954, 4489.
- 22 G. D. Smith, C. N. Caughlan, and J. A. Campell, *Inorg. Chem.*, 1972, **12**, 2989.
- 23 K. A. Mauritz, C. K. Jones, *J. Appl. Polym. Sci.*, 1990, **40**, 1402.
- 24 D. R. Payne and P. V. Wright, *Polymer*, 1982, **23**, 690.

Paper 7/03624H; Received 27th May, 1997